AGH

AGH University of Science and Technology

FACULTY OF MECHANICAL ENGINEERING AND ROBOTICS

Service Robots

Automatic Tool Change System in 3D Printers

Damian Durczok

Table of Contents

State of Art

AUTOMATIC TOOL CHANGER

An Automatic tool changer (ATC) is used in CNC machine tools to improve the production and tool carrying capacity of the machine. ATC allows a reliable method to changing the tool very quickly, reducing the non-productive time. This improves the capacity of the machine to work with a number of tools. It is one more step towards complete automation.

Where in large CNC machines this has become a standard, it is seldom come by on a smaller scale. 3D printers could greatly benefit from such a system, although it is yet to be seen.

The printing carriage has many functions to fulfill, which adds weight to an element that needs to be lightweight to allow for quick movements. An ATC could solve this problem by splitting the functionality between many heads; allowing for specialized calibration heads, printing in multiple colors and filaments, adding plotter and laser cutting functionality and even CNC milling if the frame is sturdy enough. For such a system to be practical; it needs to be fast, reliable and easy to adapt to different types of printers.

Generally automatic tool changers are customized to the provided machine and come in many shapes and forms. However, we may breakdown the ATC system to several key component modules and examine each one individually:

- Tool magazine;
- Tool transfer mechanism;
- Parking station;
- ATC arm;
- Tool clamp mechanism (spindle).

Tool Magazine

The tool magazine is responsible for storing all the tools when they are not in use. One solution is to have the tools move along a conveyor chain. The selected tool will be moved to a predetermined position from which it can be transferred by the ATC arm. This is a chain type magazine. The advantage of such a design is that the chain will conform to any path and therefore the holding capacity may be very large without taking up too much space.
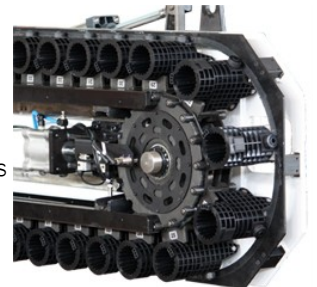
Another possible solution is a drum type magazine. Here the travel path of the tools are restricted to a circular motion. This is a much simpler design and easy to maintain and repair. Problems may occur when a large number of tools are needed, then the size of the magazine will be much larger than of the chain-type. Generally, these magazines are suitable for up to 30 tools. However, with less tool slots and a more rigid design, we can expect much faster performance compared to the chain-type magazine.

Alternatively, we may incorporate a stationary magazine. This solution requires a more complex tool transfer mechanism but greatly simplifies the magazine design. For the sake of simplicity, this will be our system of choice. The shape of the magazine will conform to the more complicated design of the ATC arm, therefore this part of the project will be designed last.

2

Tool Transfer Mechanism (TTM)

A number of methods are used to transport the tool from the magazine to the main carriage. One possible solution is to transport the actual magazine on a turret and transfer the tool directly from the turret to the head. This method severely limits tool capacity as it relies on the mechanical stability of the arm.

The other approach is to have an intermediate arm with an end effector that transfers the tool from the magazine to the head and vice versa. This is the common approach when dealing with a large number of tools. The exact transfer mechanism depends on the shape of the tool being transferred.
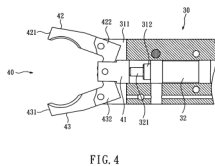
Generally, there are two school so thought for a finger based gripper mechanism.
- Pivoting movement (Link actuator);
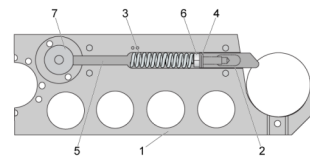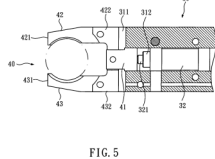- Linear or translational movement (Screw);

As well as various kinematic devices:
- Linkage actuator;
- Gear and rack actuation;
- Cam actuation;
- Screw actuation;

Below we may observe two examples:

1DOF linkage actuator gripper mechanism.

1DOF pin lock mechanism

A pivoting gripper mechanism with a screw actuator has the advantage of locking out in a single position. This will take all the forces off the motor during dynamic movement of the ATC arm. We will also design the contact surface of the gripper to be an approximate shape of the part geometry. This will provide a consistent gripping position.

Parking Station

During operation of the machine the tool change system needs to be clear of the working zone. The parking station is this region and needs to be considered during the design process.

3

ATC Arm

The arm is tasked with transporting the tool transporting mechanism. To get a better understanding of how the arm should be designed, let's look at how the mechanical portion of the tool change should work.

Sequential cycle of tool change:
1. ATC arm slides to the carriage position on linear x axis (rotates 90deg downwards, extends, enables TTM, releases tool clamp)
2. ATC arm retracts and extracts module
3. ATC arm sets module in magazine (rotates upwards, moves along x axis, extends, enables tool clamp, releases TTM, retracts)
4. ATC arm slides to the new module in the magazine (rotates, moves along x axis, extends, enables TTM, releases tool clamp, retracts)
5. ATC arm slides to the carriage position on linear x axis (rotates downwards, extends, enables tool clamp, releases TTM)
6. ATC goes back to parking station (retracts, rotates, moves along x axis)

The arm will have three degrees of motion. Linear motion along the x axis, rotational motion along its center axis and linear motion extending the arm. The tool transfer mechanism will be the fourth degree of motion in this mechanism.

Tool Clamp Mechanism

Most conventional CNC mill/lathe solutions will be insufficient for the purposes of additive manufacturing as the tools are much more varied. This mechanism will need to be completely redesigned for our purpose. It will need to fulfill four requirements to work properly.
- Sturdy tool mounting system;
- Tool clamping mechanism;
- Power and wiring to tool;
- Reliable access for tool transfer mechanism

Tool mounting system – To ensure a rigid connection between the tool and carriage, a rail system will be implemented. This will provide an easy way of attaching and removing the tool from the carriage and magazine system with minimal resistance.

Tool clamping mechanism – To prevent the tool from slipping out, a mechanism needs to be placed that locks the tool into place. A pin sliding through the rail and tool mount may be a viable option.

Power and tool wiring – Most tools will include motors and sensors. Having wires in the magazine system may create complications and therefore each tool has to be its own closed module. To supply power and wiring, the tool module will slide onto a set of pins that will supply power based on the tool attached.
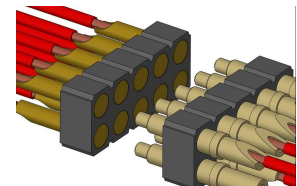
Tool transfer mechanism – A simple design that allows the tool transfer mechanism to easily grab the module.

End Effector Static Analysis

We will begin with the static analysis for the end effector.
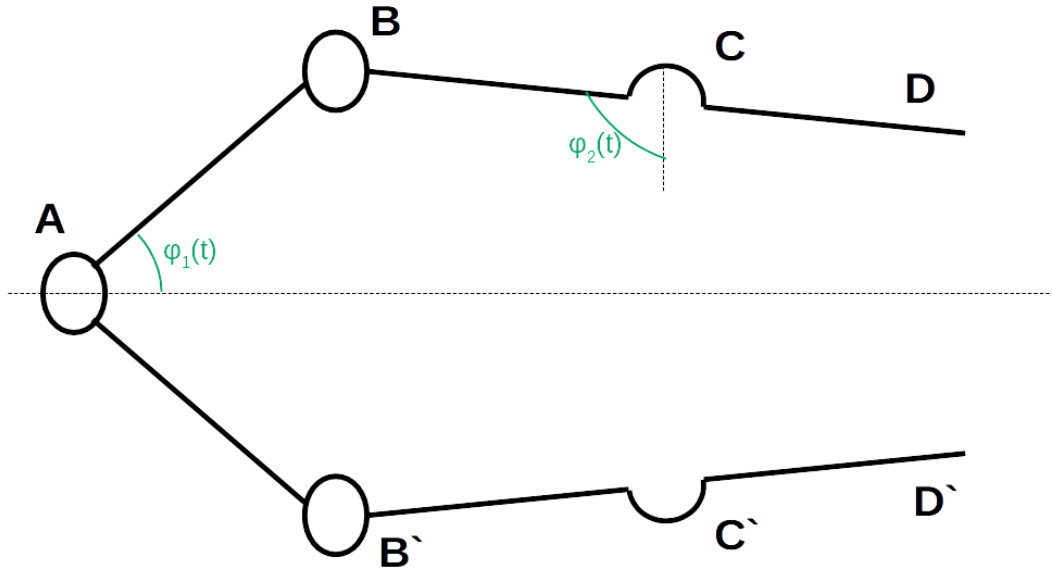
Since the end effector is symmetrical, we will only consider the top half of the mechanism. To accomodate, our P will need to be one-half the total real input force for our mechanism.

Static
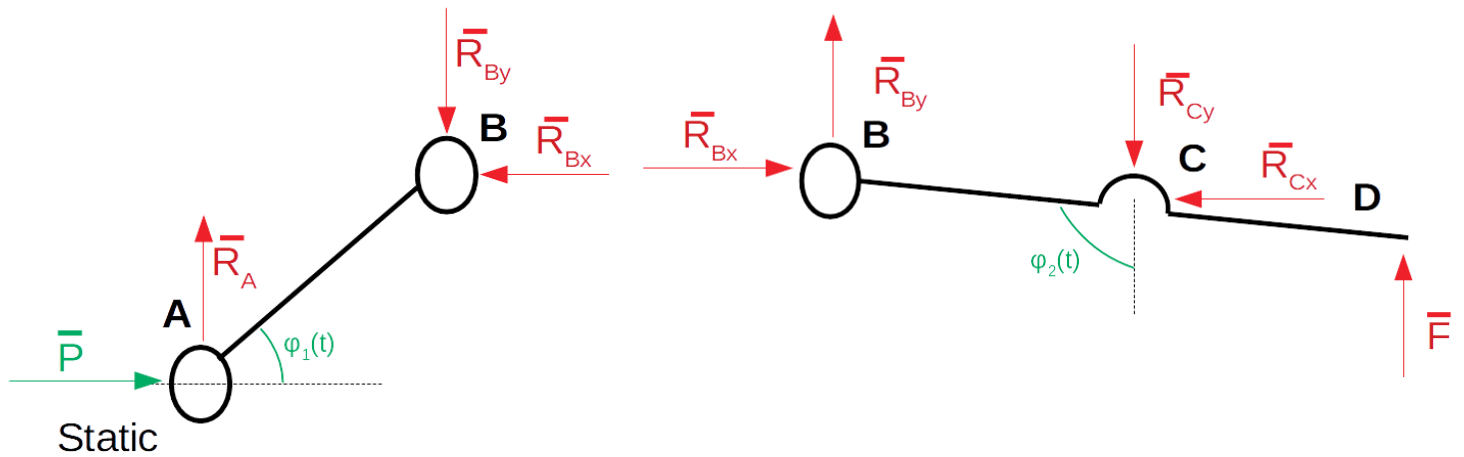
$$\begin{cases} \Sigma F_x: & P - R_{Bx} = 0 \\ \Sigma F_y: & R_A - R_{By} = 0 \\ \Sigma M_A: & l_{AB} \sin \varphi_1(t) R_{Bx} - l_{AB} \cos \varphi_1(t) R_{By} = 0 \end{cases} \Rightarrow \begin{cases} R_{Bx} = P \\ R_{By} = R_A \\ R_{By} = \tan \varphi_1(t) R_{Bx} = \tan \varphi_1(t) P \end{cases}$$

$$\begin{cases} \Sigma F_x: & R_{Bx} - R_{Cx} = 0 \\ \Sigma F_y: & R_{By} - R_{Cy} + F = 0 \\ \Sigma M_C: & -l_{BC}\cos\varphi_2(t)R_{Bx} + l_{BC}\sin\varphi_2(t)R_{By} - l_{CD}\sin\varphi_2(t)F = 0 \end{cases} \Rightarrow \begin{cases} R_{Bx} = R_{Cx} \\ F = R_{Cy} - R_{By} \\ F = \dfrac{l_{CD}}{l_{BC}}\left(R_{By} - ctg\,\varphi_2(t)R_{Bx}\right) \end{cases}$$

Final formula for the pressing force:

$$F = \frac{l_{CD}}{l_{BC}}\left(\tan\varphi_1(t) - ctg\,\varphi_2(t)\right)P$$

We may observe that the BD element functions as a lever. This may give us a mechanical advantage.

To further increase the pressing strength, we must make $\tan\varphi_1(t)$ as large as possible while minimizing $ctg\,\varphi_2(t)$. This suggests F is strongest when $\varphi_1(t) = 90^o$ and $\varphi_2(t) > 90^o$ where reasonable.

Since this formula was derived for only one-half of the end effector, we need to make a consideration to accommodate the other half. The pressing force P will remain the same, however the pressing force is now shared between two grips. Since the grips are stationary, both pressing forces must be equal and the total force is equivalent to the derived equation.

6

End Effector Velocity & Acceleration Analysis

We will begin our end effector velocity and acceleration analysis with the AB link. This consists of two basic movements; a linear movement along the x axis and a rotational movement about the point A.
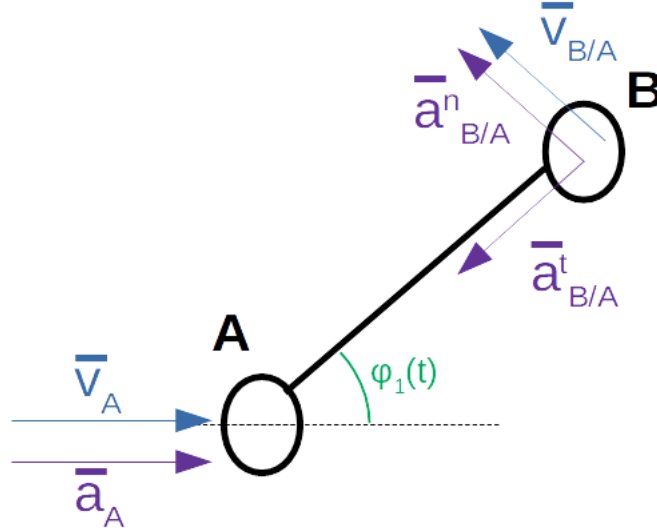
Further in the kinematic analysis, we will be examining the forces at work in the x and y axes. Therefore, we will begin our calculations by deriving the velocities and accelerations for these axes.

$$\begin{cases} \bar{v}_B = \bar{v}_A + \bar{v}_{B/A} \\ \bar{a}_B = \bar{a}_A + \bar{a}^n_{B/A} + \bar{a}^t_{B/A} \end{cases} \Rightarrow \begin{cases} v^x_B = v_A - l_{AB}\cos\varphi_1(t)\,v_{B/A} \\ v^y_B = l_{AB}\sin\varphi_1(t)\,v_{B/A} \\ a^x_B = a_A - l_{AB}\cos\varphi_1(t)\,a^n_{B/A} - l_{AB}\cos\varphi_1(t)\,a^t_{B/A} \\ a^y_B = l_{AB}\sin\varphi_1(t)\,a^n_{B/A} - l_{AB}\sin\varphi_1(t)\,a^t_{B/A} \end{cases}$$

The following relations are needed to further simplify the equations.

$$\begin{cases} v_{B/A} = l_{AB}\,\dot{\varphi}_1(t) \\ a^n_{B/A} = l_{AB}\,\ddot{\varphi}_1(t) \\ a^t_{B/A} = l_{AB}\,\dot{\varphi}^2_1(t) \end{cases}$$

We end up with these four equations for the point B:

$$\begin{cases} v^x_B = v_A - l^2_{AB}\,\dot{\varphi}_1(t)\cos\varphi_1(t) \\ v^y_B = l^2_{AB}\sin\dot{\varphi}_1(t)\varphi_1(t) \\ a^x_B = a_A - l^2_{AB}\,\ddot{\varphi}_1(t)\cos\varphi_1(t) - l^2_{AB}\,\dot{\varphi}^2_1(t)\cos\varphi_1(t) \\ a^y_B = l^2_{AB}\,\ddot{\varphi}_1(t)\sin\varphi_1(t) - l^2_{AB}\,\dot{\varphi}^2_1(t)\sin\varphi_1(t) \end{cases}$$

Any further computations of velocities or accelerations will be with the use of these equations with some slight modifications explained later.

We may notice that the results depend on a few variables; velocities and accelerations at point A, angle orientation of link AB and the distance between point A and B. If we where to choose any other point along the link AB, the velocities and accelerations at point A and the angle orientation of link AB will be the same. The only difference will be the distance between point A and the new chosen point. Therefore, the required modification of the equations is to simply replace the constant distance (l) and we will obtain a new set of equations for any given point.

Next we may relate the above equations to the link BD. With B being a shared joint between the two, the velocities and accelerations are shared at point B. The link BD only exhibits rotary motions. We will need to derive the angular velocities and accelerations.
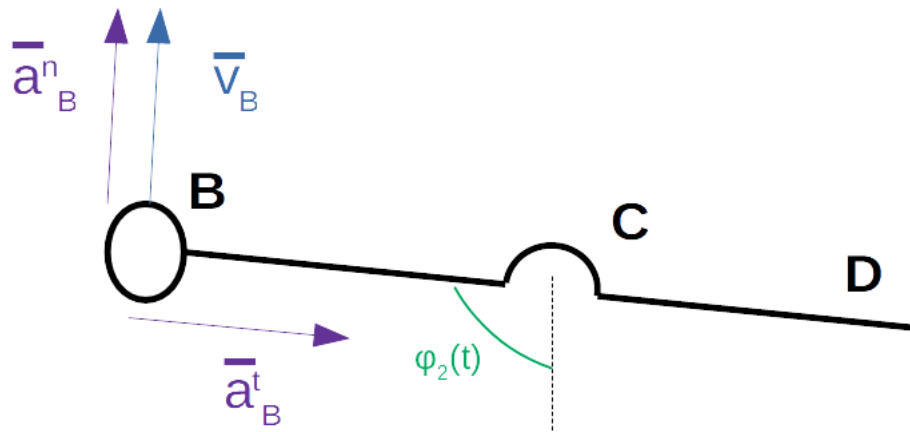
The angular velocity of the link BD : $\dot{\varphi}_2(t) = \dfrac{v_B}{l_{BC}}$

The angular acceleration of link BD : $\ddot{\varphi}_2(t) = \dfrac{a_B}{l_{BC}}$

To obtain the exact values of v_B and a_B , one more set of formulas are require.

$$\begin{cases} v_B = \sqrt{(v_B^x)^2 + (v_B^y)^2} \\ a_B = \sqrt{(a_B^x)^2 + (a_B^y)^2} \end{cases}$$
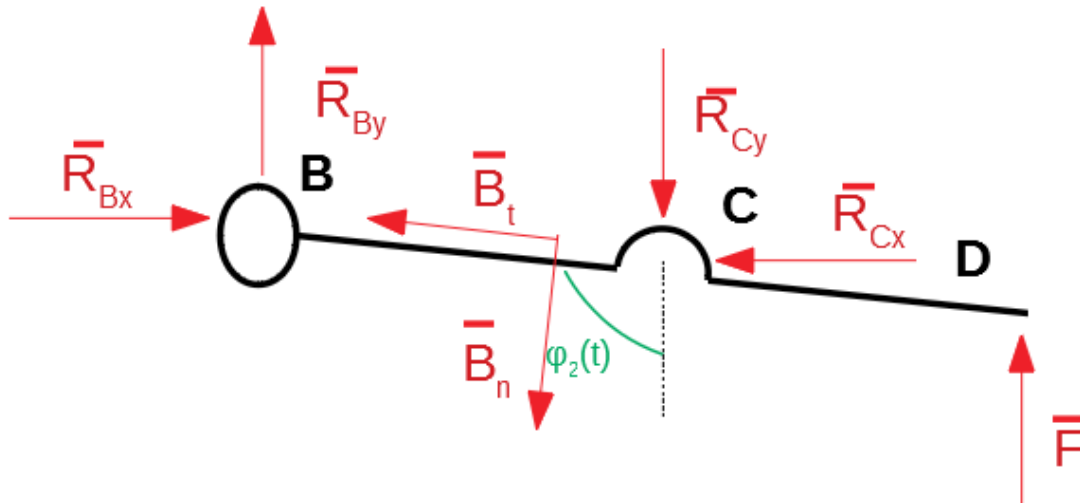
At this point, the calculations are getting much more time consuming. Programs such as Matlab will speed up this process and is less error prone to traditional hand calculations.

8

End Effector Dynamic Analysis
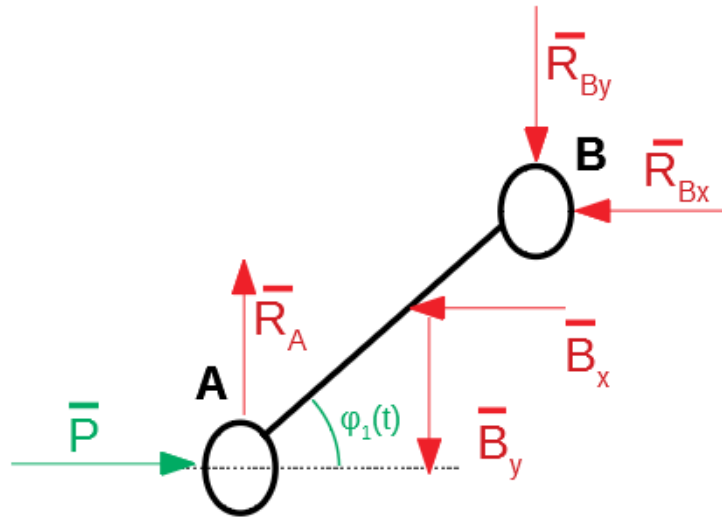
$$\begin{cases} \Sigma F_x: & P - R_{Bx} - B_x = 0 \\ \Sigma F_y: & R_A - R_{By} - B_y = 0 \\ \Sigma M_A: & l_{AB} \sin\varphi_1(t) R_{Bx} - l_{AB} \cos\varphi_1(t) R_{By} - l_{Acm} \sin\varphi_1(t) B_x - l_{Acm} \cos\varphi_1(t) B_y = 0 \end{cases}$$

$$\Rightarrow \begin{cases} R_{Bx} = P - B_x \\ R_A - R_{By} = B_y \\ l_{AB} \tan\varphi_1(t) R_{Bx} - l_{AB} R_{By} = l_{Acm} B_y - l_{Acm} \tan\varphi_1(t) B_x \end{cases}$$

$$\begin{cases} \Sigma F_x: & R_{Bx} - R_{Cx} - \sin\varphi_2(t) B_t^x + \cos\varphi_2(t) B_n^x = 0 \\ \Sigma F_y: & R_{By} - R_{Cy} + F - \cos\varphi_2(t) B_t^y - \sin\varphi_2(t) B_n^y = 0 \\ \Sigma M_C: & -l_{BC} \cos\varphi_2(t) R_{Bx} + l_{BC} \sin\varphi_2(t) R_{By} - l_{CD} \sin\varphi_2(t) F + l_{Bcm} B_n = 0 \end{cases}$$

9

$$\Rightarrow \begin{cases} R_{Bx} - R_{Cx} = \sin\varphi_2(t) B_t^x - \cos\varphi_2(t) B_n^x \\ R_{By} - R_{Cy} = \cos\varphi_2(t) B_t^y + \sin\varphi_2(t) B_n^y - F \\ -l_{BC}\cos\varphi_2(t) R_{Bx} + l_{BC}\sin\varphi_2(t) R_{By} = l_{Bcm} B_n - l_{CD}\sin\varphi_2(t) F \end{cases}$$

The inertial force vectors were chosen based on the previous analysis of accelerations.

Next we will put the formulas in matrix form so they may be used in Matlab.

$$\begin{bmatrix} 0 & 1 & 0 & 0 & 0 \\ 1 & 0 & -1 & 0 & 0 \\ 0 & l_{AB}\tan\varphi_1(t) & -l_{AB} & 0 & 0 \\ 0 & 1 & 0 & -1 & 0 \\ 0 & 0 & 1 & 0 & -1 \\ 0 & -l_{BC}\cos\varphi_2(t) & l_{BC}\sin\varphi_2(t) & 0 & 0 \end{bmatrix} \begin{bmatrix} R_A \\ R_{Bx} \\ R_{By} \\ R_{Cx} \\ R_{Cy} \end{bmatrix} = \begin{bmatrix} P \\ 0 \\ 0 \\ 0 \\ -F \\ -l_{CD}\sin\varphi_2(t) F \end{bmatrix} + \begin{bmatrix} -B_x \\ B_y \\ l_{Acm} B_y - l_{Acm}\tan\varphi_1(t) B_x \\ \sin\varphi_2(t) B_t^x - \cos\varphi_2(t) B_n^x \\ \cos\varphi_2(t) B_t^y + \sin\varphi_2(t) B_n^y \\ l_{Bcm} B_n \end{bmatrix}$$

To further reduce the number of variables, we may relate the two angles $\varphi_1(t)$ and $\varphi_2(t)$.
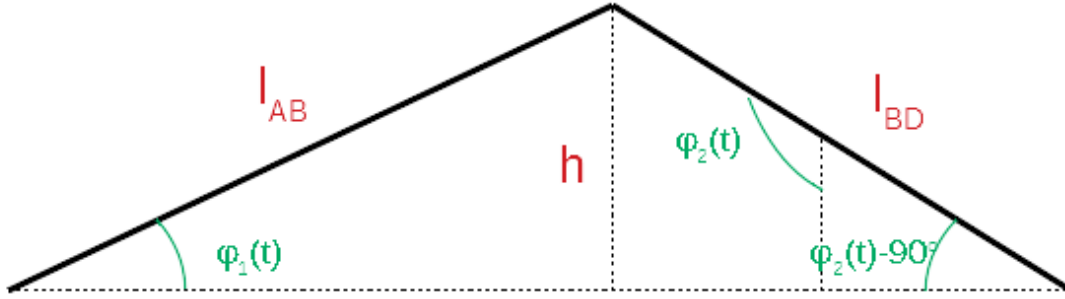
$$\begin{cases} \sin\varphi_1(t) = \dfrac{h}{l_{AB}} \\ \sin(\varphi_2(t) - 90) = \dfrac{h}{l_{BD}} \end{cases} \quad \Rightarrow \quad l_{AB}\sin\varphi_1(t) = l_{BD}\cos\varphi_2(t) \quad \Rightarrow \quad \varphi_2(t) = arcos\left(\dfrac{l_{AB}}{l_{BD}}\sin\varphi_1(t)\right)$$

For a static analysis we may exclude the inertial force matrix. This static analysis is only sufficient for when the gripper mechanism including the arm is stationary. The same applies for the dynamic analysis as any kinematics of the arm aren't included.

As the clamping strength of the end effector while the arm is in motion is an integral part of contraption, these calculations do not fully represent the behavior of the entire system. The next part of the analysis will include the dynamics of the next three degrees of freedom.

10

Arm Kinematics

The next part of the analysis is the ATC arm. The arms responsibility is to position the end effector gripper in the correct position. Below is the kinematic chain of the arm.
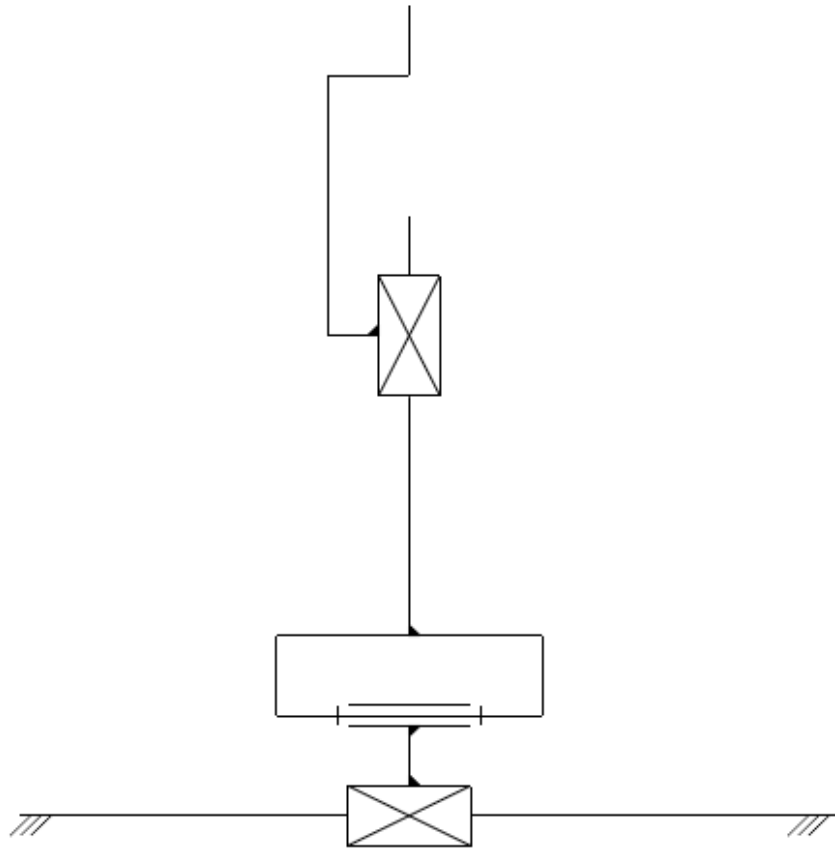
The manipulator is comprised of 3 class V kinematic pairs. We may now use the equation for the number of degrees of freedom: $w = 6n - \sum_{i=1}^{5} ip_i$ where,

w — number of degrees of freedom
n — number o movable links
pi — number of pairs of class i

$w = 6*3 - 5*3 = 3$, we conclude that our system has three degrees of freedom.

The first degree of freedom will mimic the Cartesian styled machine in the x-axis. It is responsible for manoeuvring to the correct location in the magazine. The second motion is rotational, which is responsible for leaving the magazine area and into the head change zone. The final degree of freedom is once again linear. This final movement is what will be applying and removing the tools. The final element will be the end effector, which will only add one more degree of motion to our complete system.
We will be using the Denavit-Hartenberg notation to calculate the **forward kinematics** of our ATC arm.
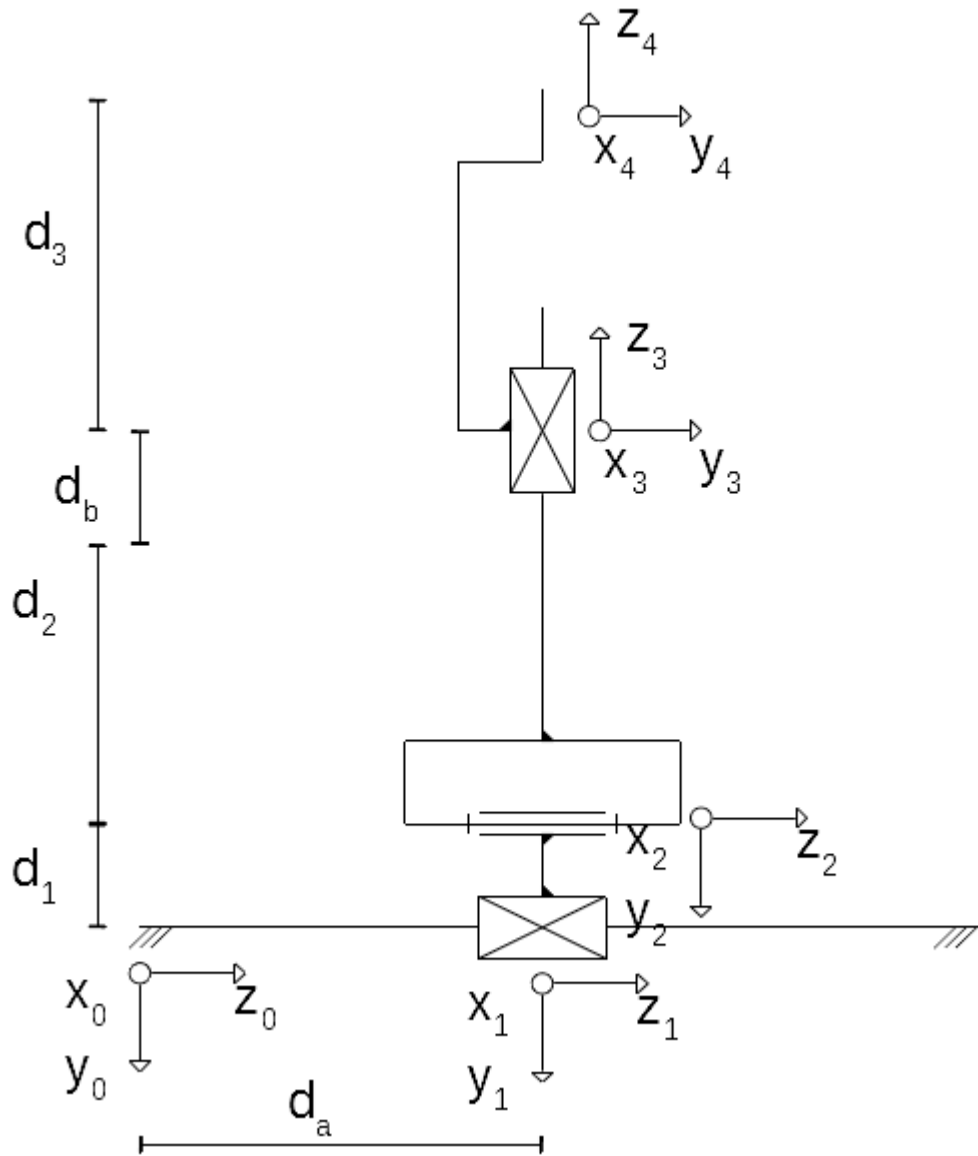
		θ_i	d_i	a_i	α_i
1		0	$d_{a,var}$	0	90
2		0	d_1	0	-90
3		$\theta_{1,var}$	0	0	90
4		0	$d_{b,var}+d_2$	0	0
5		0	d_3	0	0

The main formula is below

$$A_i = Rot_{z,\theta_i} \, Trans_{z,d_i} \, Trans_{x,a_i} \, Rot_{x,\alpha_i} =$$

$$= \begin{bmatrix} \cos(\theta_i) & -\sin(\theta_i) & 0 & 0 \\ \sin(\theta_i) & \cos(\theta_i) & 0 & 0 \\ 0 & 0 & 1 & 0 \\ 0 & 0 & 0 & 1 \end{bmatrix} \begin{bmatrix} 1 & 0 & 0 & 0 \\ 0 & 1 & 0 & 0 \\ 0 & 0 & 1 & d_i \\ 0 & 0 & 0 & 1 \end{bmatrix} \begin{bmatrix} 1 & 0 & 0 & a_i \\ 0 & 1 & 0 & 0 \\ 0 & 0 & 1 & 0 \\ 0 & 0 & 0 & 1 \end{bmatrix} \begin{bmatrix} 1 & 0 & 0 & 0 \\ 0 & \cos(\alpha_i) & -\sin(\alpha_i) & 0 \\ 0 & \sin(\alpha_i) & \cos(\alpha_i) & 0 \\ 0 & 0 & 0 & 1 \end{bmatrix}$$

We will begin by calculating all five A matrices separately.

$$A_1 = Trans_{z,d_{a,var}} Rot_{x,90} = \begin{bmatrix} 1 & 0 & 0 & 0 \\ 0 & 1 & 0 & 0 \\ 0 & 0 & 1 & d_{b,var} \\ 0 & 0 & 0 & 1 \end{bmatrix} \begin{bmatrix} 1 & 0 & 0 & 0 \\ 0 & \cos(90) & -\sin(90) & 0 \\ 0 & \sin(90) & \cos(90) & 0 \\ 0 & 0 & 0 & 1 \end{bmatrix} = \begin{bmatrix} 1 & 0 & 0 & 0 \\ 0 & 0 & -1 & 0 \\ 0 & 1 & 0 & d_{a,var} \\ 0 & 0 & 0 & 1 \end{bmatrix}$$

$$A_2 = Trans_{z,d_1} Rot_{x,-90} = \begin{bmatrix} 1 & 0 & 0 & 0 \\ 0 & 1 & 0 & 0 \\ 0 & 0 & 1 & d_1 \\ 0 & 0 & 0 & 1 \end{bmatrix} \begin{bmatrix} 1 & 0 & 0 & 0 \\ 0 & \cos(-90) & -\sin(-90) & 0 \\ 0 & \sin(-90) & \cos(-90) & 0 \\ 0 & 0 & 0 & 1 \end{bmatrix} = \begin{bmatrix} 1 & 0 & 0 & 0 \\ 0 & 0 & 1 & 0 \\ 0 & -1 & 0 & d_1 \\ 0 & 0 & 0 & 1 \end{bmatrix}$$

$$A_3 = Rot_{z,\theta_{1,var}} Rot_{x,90} = \begin{bmatrix} \cos(\theta_{1,var}) & -\sin(\theta_{1,var}) & 0 & 0 \\ \sin(\theta_{1,var}) & \cos(\theta_{1,var}) & 0 & 0 \\ 0 & 0 & 1 & 0 \\ 0 & 0 & 0 & 1 \end{bmatrix} \begin{bmatrix} 1 & 0 & 0 & 0 \\ 0 & \cos(90) & -\sin(90) & 0 \\ 0 & \sin(90) & \cos(90) & 0 \\ 0 & 0 & 0 & 1 \end{bmatrix} =$$

$$= \begin{bmatrix} \cos(\theta_{1,var}) & 0 & \sin(\theta_{1,var}) & 0 \\ \sin(\theta_{1,var}) & 0 & -\cos(\theta_{1,var}) & 0 \\ 0 & 1 & 0 & 0 \\ 0 & 0 & 0 & 1 \end{bmatrix}$$

$$A_4 = Trans_{z,d_{b,var}+d_2} \begin{bmatrix} 1 & 0 & 0 & 0 \\ 0 & 1 & 0 & 0 \\ 0 & 0 & 1 & d_{b,var}+d_2 \\ 0 & 0 & 0 & 1 \end{bmatrix}$$

$$A_5 = Trans_{z,d_3} \begin{bmatrix} 1 & 0 & 0 & 0 \\ 0 & 1 & 0 & 0 \\ 0 & 0 & 1 & d_3 \\ 0 & 0 & 0 & 1 \end{bmatrix}$$

13

$$A_{5,0}=A_1 A_2 A_3 A_4 A_5=\begin{bmatrix} 1 & 0 & 0 & 0 \\ 0 & 1 & 0 & -d_1 \\ 0 & 0 & 1 & d_{a,var} \\ 0 & 0 & 0 & 1 \end{bmatrix} A_3 A_4 A_5 = \begin{bmatrix} \cos(\theta_{1,var}) & 0 & \sin(\theta_{1,var}) & 0 \\ \sin(\theta_{1,var}) & 0 & -\cos(\theta_{1,var}) & -d_1 \\ 0 & 1 & 0 & d_{a,var} \\ 0 & 0 & 0 & 1 \end{bmatrix} A_4 A_5 =$$

$$= \begin{bmatrix} \cos(\theta_{1,var}) & 0 & \sin(\theta_{1,var}) & (d_{b,var}+d_2)\sin(\theta_{1,var}) \\ \sin(\theta_{1,var}) & 0 & -\cos(\theta_{1,var}) & -(d_{b,var}+d_2)\cos(\theta_{1,var})-d_1 \\ 0 & 1 & 0 & d_{a,var} \\ 0 & 0 & 0 & 1 \end{bmatrix} =$$

$$= \begin{bmatrix} \cos(\theta_{1,var}) & 0 & \sin(\theta_{1,var}) & (d_{b,var}+d_2+d_3)\sin(\theta_{1,var}) \\ \sin(\theta_{1,var}) & 0 & -\cos(\theta_{1,var}) & -(d_{b,var}+d_2+d_3)\cos(\theta_{1,var})-d_1 \\ 0 & 1 & 0 & d_{a,var} \\ 0 & 0 & 0 & 1 \end{bmatrix}$$

$$A_{5,0} = \begin{bmatrix} \cos(\theta_{1,var}) & 0 & \sin(\theta_{1,var}) & (d_{b,var}+d_2+d_3)\sin(\theta_{1,var}) \\ \sin(\theta_{1,var}) & 0 & -\cos(\theta_{1,var}) & -(d_{b,var}+d_2+d_3)\cos(\theta_{1,var})-d_1 \\ 0 & 1 & 0 & d_{a,var} \\ 0 & 0 & 0 & 1 \end{bmatrix}$$

To check if our equations make any physical sense, we may substitute some parameters.

Let $d_1, d_2, d_3, d_a, d_b = 2$ and $\theta_1 = 0$;

so, $A_{5,0} = \begin{bmatrix} 1 & 0 & 0 & 0 \\ 0 & 0 & -1 & -8 \\ 0 & 1 & 0 & 2 \\ 0 & 0 & 0 & 1 \end{bmatrix}$

The position matrix shows us that the coordinates of the end effector are (0, -8, 2) with respect to the original coordinate system, which are the anticipated results. Similarly, the rotation matrix shows that the new Y axis is in the orientation of the old Z axis and the new Z axis took the orientation of the old Y in the opposite direction.

Based on this quick analysis, we may conclude that our calculations are correct and we may progress to the **inverse kinematics**.

$$\begin{cases} x = (d_{b,var}+d_2+d_3)\sin(\theta_{1,var}) \\ y = -(d_{b,var}+d_2+d_3)\cos(\theta_{1,var})-d_1 \\ z = d_{a,var} \end{cases}$$

14

Solving for $\theta_{1,var}$:
$$\frac{x}{\sin(\theta_{1,var})}-d_2-d_3=-\frac{y+d_1}{\cos(\theta_{1,var})}-d_2-d_3$$

$$x\cos(\theta_{1,var})=-\sin(\theta_{1,var})(y+d_1)$$

$$\frac{\sin(\theta_{1,var})}{\cos(\theta_{1,var})}=-\frac{x}{y+d_1}$$

$$tg(\theta_{1,var})=-\frac{x}{y+d_1}$$

$$\theta_{1,var}=tg^{-1}\left(-\frac{x}{y+d_1}\right)=-tg^{-1}\left(\frac{x}{y+d_1}\right)$$

Solving for $d_{b,var}$:
$$d_{b,var}=\frac{x}{\sin(\theta_{1,var})}-d_2-d_3$$

$$d_{b,var}=-\left(\frac{x}{\sin\left(tg^{-1}\left(\frac{x}{y+d_1}\right)\right)}+d_2+d_3\right)$$

$$d_{b,var}=-\left(\frac{x}{\dfrac{\dfrac{x}{y+d_1}}{\sqrt{1+\dfrac{x^2}{(y+d_1)^2}}}}+d_2+d_3\right)$$

$$d_{b,var}=-\left(\frac{y+d_1}{\sqrt{1+\dfrac{x^2}{(y+d_1)^2}}}+d_2+d_3\right)$$

Solving for $d_{a,var}$:
$$d_{a,var}=z$$

Below we may see that the derived equations are valid based on the previously chosen parameters:

$$\begin{cases}\theta_{1,var}=-tg^{-1}\left(\dfrac{x}{y+d_1}\right)\\[2mm]d_{b,var}=-\left(\dfrac{y+d_1}{\sqrt{1+\dfrac{x^2}{(y+d_1)^2}}}+d_2+d_3\right)\\[2mm]d_{a,var}=z\end{cases}\Rightarrow\begin{cases}\theta_{1,var}=-tg^{-1}\left(\dfrac{0}{-8+2}\right)=0\\[2mm]d_{b,var}=-\left(\dfrac{-8+2}{\sqrt{1+\dfrac{0^2}{(-8+2)^2}}}+2+2\right)=2\\[2mm]d_{a,var}=2\end{cases}$$

15

Rack and Pinion

For the x axis linear movement we will be using a rack and pinion setup. The fact that this particular linear motion only serves the purpose of locating elements in the magazine means that speed and acceleration isn't a priority. Precision and accuracy is much more preferred.

The rack and pinions advantage over the belt drive is that the belt needs to be properly tensioned and is used for high speed tasks. Another possible solution is to use a linear ball screw drive, however there is a certain geometrical constraint that prevents the use of such mechanism. This will be reviewed once again during the CAD design.

To select the correct rack and pinion for the x axis linear movement, we will make a few assumptions and calculations.

Mass to be Moved	m	= 5 kg
Speed	v	= 1 m/s
Acceleration Time	t_b	= 1 s
Acceleration Due to Gravity	g	= 9.81 m/s2
Coefficient of Friction	μ	= 0.15
Load Factor	K_A	= 1
Life-Time Factor	f_n	= 0.85
Safety Coefficient	S_B	= 1.3
Linear Load Distribution Factor	$L_{KH\beta}$	= 1.5

Calculations:

$$a = \frac{v}{t_b} = \frac{1}{1} = 1\frac{m}{s^2}$$

$$F_u = \frac{m*g*\mu + m*a}{1000} = \frac{12.3575}{1000} = 0.0123575\,kN$$

The tangential force acting between our rack and pinion is quite small. We will now select an appropriate pinion and rack from a catalogue with a slightly larger feed force and compare the two values.

Assumed feed force:
rack BR(Basic Rack) C45, ind. hardened, straight tooth, module 1, (25 10 050)
pinion C45, Ind. Hardened, 20 teeth, (21 10 020), page ZB-36 F_{utab} = 1 kN

$$F_{u\,zul./per.} = \frac{F_{uTab}}{K_A*S_B*f_n*L_{KH\beta}} = \frac{1}{1.6575} = 0.6\,kN$$

Condition:
$$F_{u\,zul./per.} > F_u \qquad\qquad 0.6\,kN > 0.0123575\,kN$$

With the above condition satisfied, we know that the rack and pinion will be sufficient for our application. However it is 50 times above our minimum value. A less industrial approach, such a plastic rack and pinion from a 3d printer may prove to be satisfactory at a much lower cost.

Belt Drive

The rotary joint is responsible for aligning the end-effector either in position to access the magazine or the x-carriage. This joint will be belt driven to provide the necessary output torque and fit in a compact design.

The calculations for the output torque of an open belt configuration are quite simple. First assumptions need to be made. Since a belt can only provide a pulling force and not a pushing one to drive a pulley, we may expect one side of the belt to have slack and the other to be tight. However, we will assume this is not happening in our case and that all points on the belt are moving with equal velocity.

Open Belt Configuration
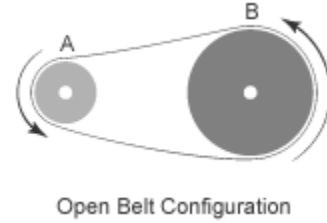
If all points on the belt are moving with equal velocity, so are the outer points on the pulleys. Therefore the following system of equations may be created.

$$\begin{cases} v_A = \omega_A d_A \\ v_B = \omega_B d_B \\ v_A = v_B \end{cases} \Rightarrow \omega_B = \omega_A \frac{d_A}{d_B}$$

Now we have a relationship of angular velocities between the two pulleys.

To derive the torque transmission we may refer to the conservation of energy.

$$\begin{cases} P_A = T_A \omega_A \\ P_B = T_B \omega_B \\ P_A = P_B \end{cases} \Rightarrow T_B = T_A \frac{\omega_A}{\omega_B}$$

If we relate both of our derived equations we get the following.

$$T_B = T_A \frac{d_B}{d_A}$$

Where $\dfrac{d_B}{d_A}$ is the gear/pulley ratio. The entire formula may be summed up nicely like so.

Motor Torque x Gear/Pulley Ratio = Torque Output

We want our arm to be able to handle 0.5kg(5N) at a distance of 20cm. This will provide a moment of 100Ncm.

Our design may incorporate a 15mm diameter driving pulley and a 45mm driven pulley. A Nema17 motor with a holding torque of 42Ncm will output a torque of 126Ncm on the pulley. This fulfills our requirements.

Lead Screw Drive

The linear extension movement will be produced by a lead screw drive and a guide rail system.

Let us assume we will be using a 4 lead M6 lead screw with a thread density of 52 threads per 10cm. Meaning to translate an object 1 cm, we need to rotate the screw 1.3 times.

We will be using the work energy theorem to calculate the torque needed to lift this weight.

Work needed to be done to lift the object:

$$mgh_1 + W_h + W_{other} = mgh_2$$

,where $F = mg$ is the force of the object due to gravitational acceleration

W_h is the energy needed to change the object height

$W_{other} = -\mu F_n \Delta h$ is the energy lost due to friction

After reconfiguring our equation, we get the following:

$$W_h = F \Delta h + \mu F_n \Delta h$$

Work needed to be done to rotate the lead screw an angle of θ:

$$W_\theta = \tau \Delta \theta$$

,where W_θ is the energy needed to rotate the lead screw

$\Delta \theta$ is the angle of rotation

τ is the torque of the motor

Relationship between Δh and $\Delta \theta$:

$$\Delta h (1.3) = \Delta \theta$$

With the above relationship, we now know how the raise height is dependent on the angle of rotation of the lead screw. Therefore we can compare the energy needed to rotate the shaft to the energy needed to lift the shaft.

If we combine the three above equations, we get the following:

$$\tau = \frac{1}{1.3}(F + \mu F_n)$$

Since we want to know the maximum torque we need supplied by our motor, we need to find when the potential energy is increasing. Therefore the maximum torque required by our motor will be encountered when the arm is pointing downwards and is being raised. We will now only examine this one scenario.

Since the motion is strictly vertical, we know that the normal force of friction is parallel to the lead screw, more specifically we know that it is equal to F . This gives us the new equation:

$$\tau = \frac{F(1+\mu)}{1.3} \quad \text{in} \quad [Ncm]$$

and the result:

$$\tau = \frac{5(1+0.3)}{1.3} = 5 \, Ncm$$

With such a low torque, we may use a DC motor to drive the screw.

CAD

Below is the CAD model of the first iteration. The model was designed using Siemens NX software. Siemens NX provides built in simulation software for gcode drive and ATC systems. It is also a powerful 3D modeling software that provides an efficient environment for this project.

This iteration was specifically designed to fit in a previously created 3D printer. Based on the previous calculations, we are using two stepper motors and two dc motors. The stepper motors drive the first two degrees of freedom from the base, the linear and rotational movement, which are responsible for positioning the endeffector. The stepper motors provide precision and accuracy. To calibrate the stepper motors, two endstop switches are needed. One for the linear axis and the other for the rotary. A pololu stepper driver will be responsible for driving these motors.

The other two motors simply change between two states. The first motor is either extended or recessed and the other one is either clamped or not. This makes the use of precise stepper motors redundent. We may either use an encoder or somesort of sensor for these motors to determine the current state.
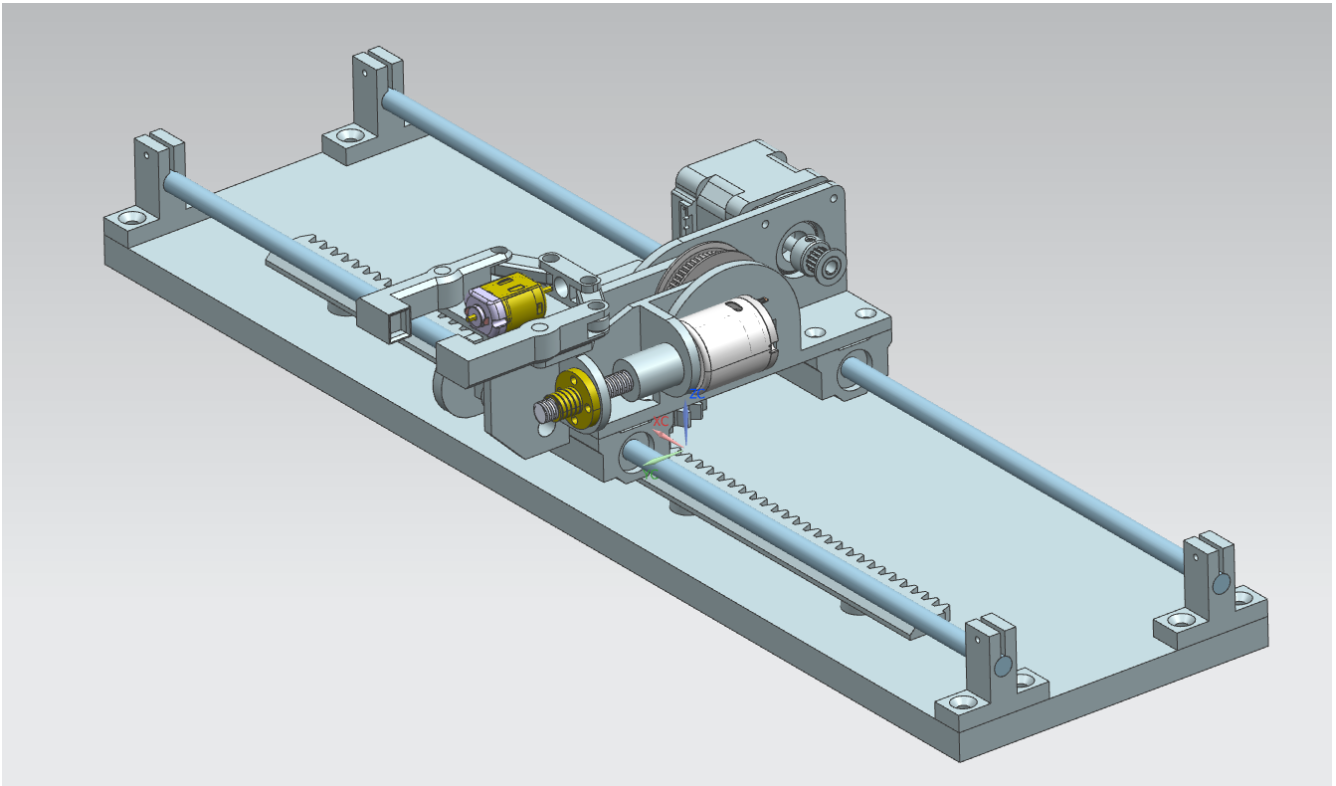

We use an assortment of bearings to constrain the movements. The first bearings for the lateral linear movement are sma08uu linear bearings which come within an enclosure. This allows for easy replacement of these parts and makes the construction of the arm more convenient. The rails are standard 8mm smooth rods.

For the next rotary movement, we use two 623zz bearings and a shaft. The pulleys are also standard parts described in the earlier calculations. Following this movement we have a linear extension movement. This is guided by a rail and once again two 623zz bearings. Their small dimensions are an attribute to the compact design.

Different angles of the CAD design.
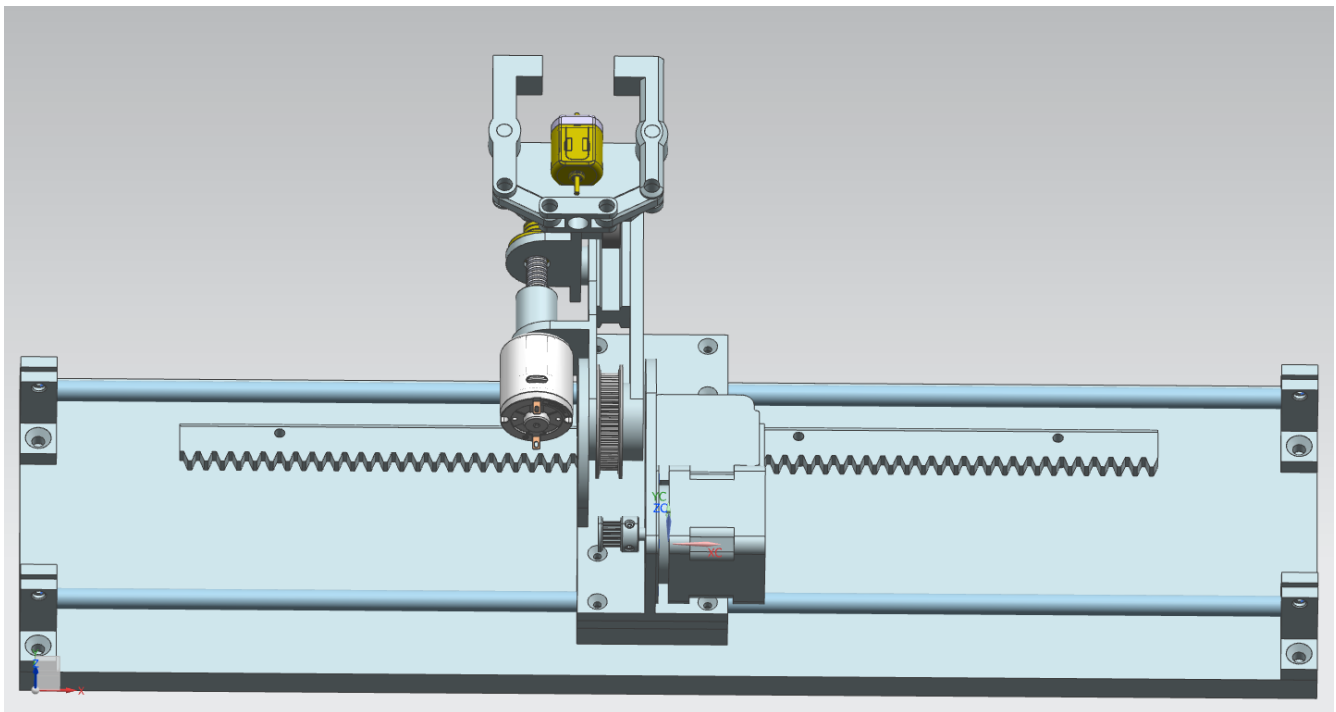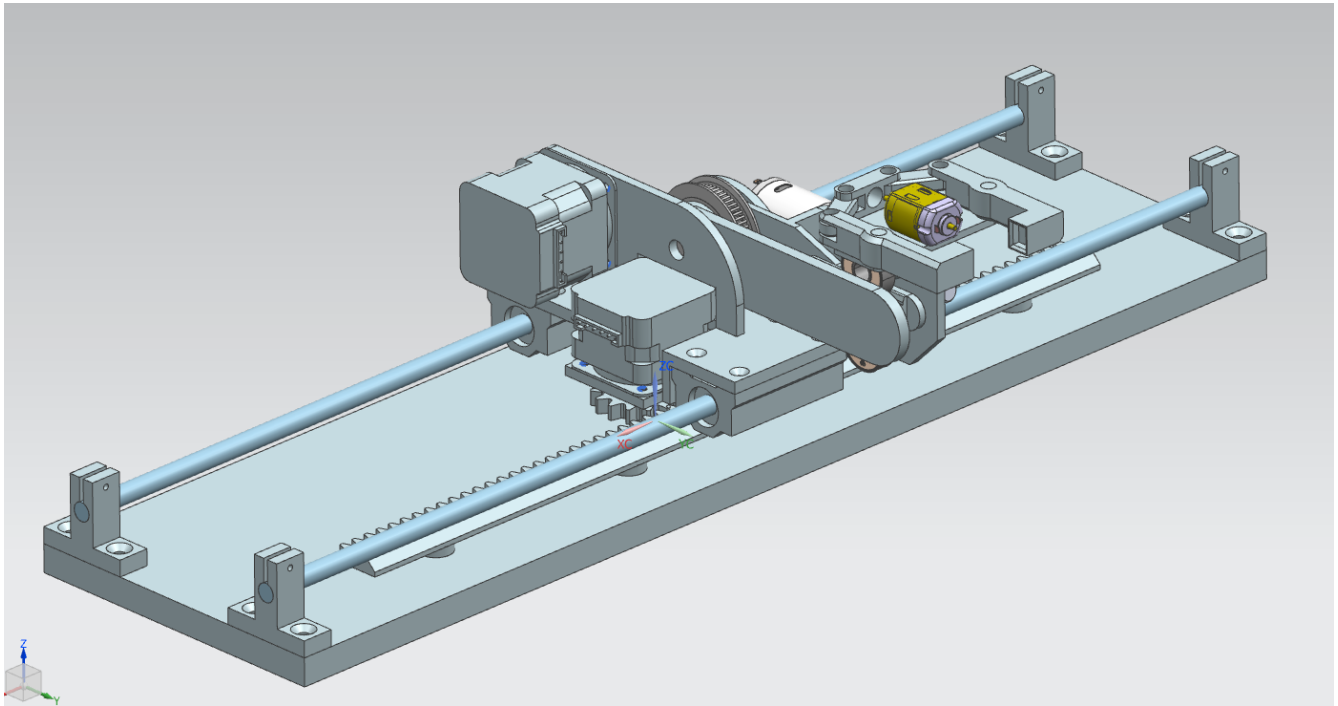
The final image shows the ATC implemented in the machine.
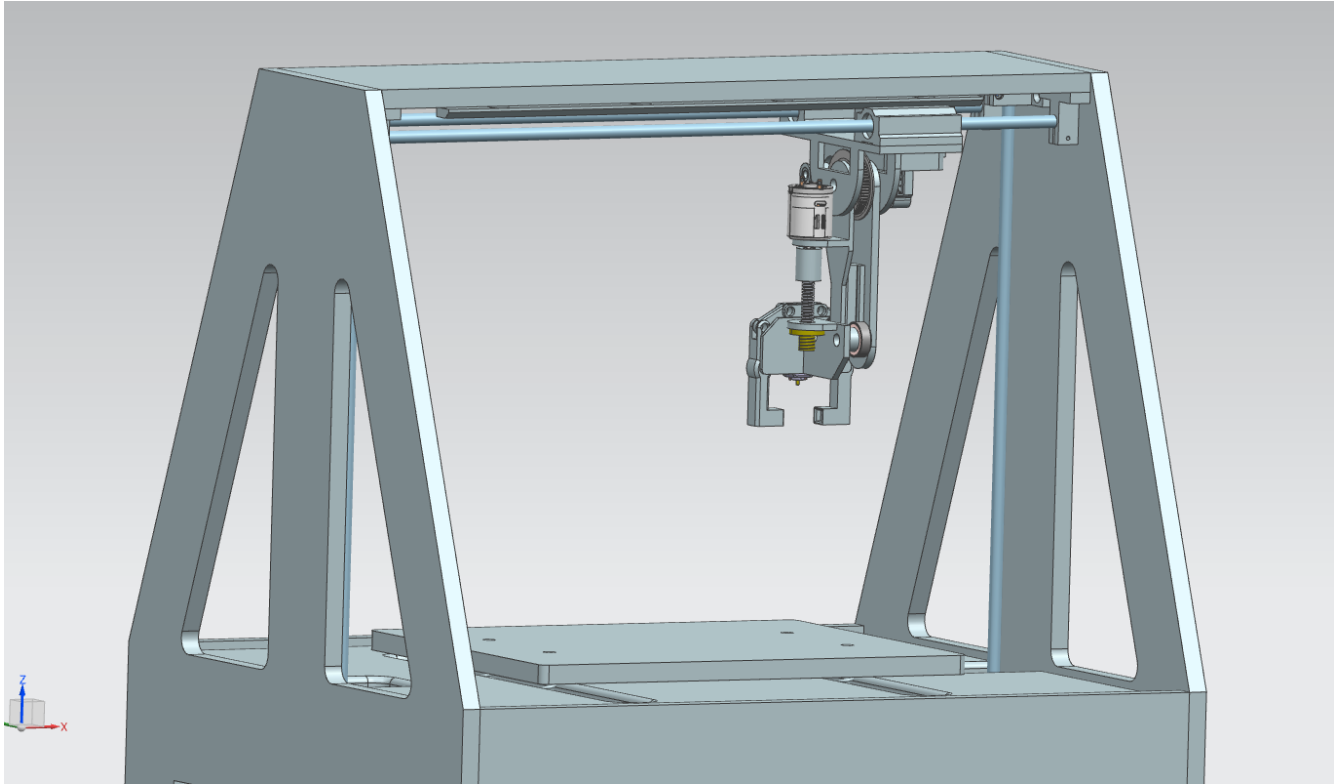
d

SOURCES:

Ed. B. Katalinic, (2012), DESIGN OF AN AUTOMATIC TOOL CHANGER SYSTEM FOR MILLING MACHINING CENTERS, Published by DAAAM International, Vienna, Austria, EU,

FADAL USER MANUAL, (2003), pp. 113-184

Jernej Prešeren, Dejan Avguštin, Tadej Mravlje, (2005), GUIDELINES FOR THE DESIGN OF ROBOTIC GRIPPING SYSTEM, Ljubljana, Sloveni